Available online at www.sciencedirect.com

ScienceDirect

Chinese Journal of Aeronautics 22(2009) 644-648

Chinese Journal of Aeronautics

www.elsevier.com/locate/cja

Design and Experiments of Model-free Compound Controller of Flight Simulator

Guo Zhifu*, Cao Jian, Zhao Keding

School of Mechatronic Engineering, Harbin Institute of Technology, Harbin 150001, China

Received 29 October 2008; accepted 12 January 2009

Abstract

A model-free compound controller design method is proposed to achieve the wide frequency bandwidth requirement of flight simulators. The method based on quantitative feedback theory, acquires system uncertainty under different working conditions through closed-loop identification with power spectrum estimation. Then in controller designing, it makes a tradeoff between the strict requirements for magnitude-frequency characteristics and those for phase-frequency characteristics of flight simulators, by converting the indices of magnitude-frequency characteristics of flight simulators into quantitative feedback theory-based tracking specification bounds and using feedforward controller to attain the required phase-frequency characteristics. Simulation and experimental results indicate that, when used to design inner frame controller of flight simulator, the proposed method can fulfill the requirements for wide frequency bandwidth indices. Compared with other controller design methods, it has the property of model-free and transparency.

Keywords: model-free; quantitative feedback theory; power spectrum estimation; flight simulators; closed-loop system identification

1. Introduction

The flight simulator is one of the key equipment for hardware-in-the-loop (HWIL) simulation, which can be used to verify performance indices of sensors, guidance systems, control systems and actuators. With unabated advancement of unit under test, wider frequency bandwidth of flight simulators that influences dynamic characteristic testing is required. The two main factors that decide frequency bandwidth of flight simulators, as it is known, are motor power and structure rigidity[1].

At present, the research on widening frequency bandwidth of flight simulators mainly concentrates on improving the control strategies on the assumption that motor power and structure rigidity have met requirements of simulators. Z. M. Li, et al.[2] introduced command shaping technique to suppress vibration and expand frequency bandwidth of flight simulators. L. A. DeMore, et al.[3] presented a state variable feedback control system architecture with feedforward techniques to improve the flight table's dynamic fidelity by significantly reducing the table's low frequency phase lag. M. Swamp, et al.[4] used acceleration feedback as a part of the axes servo system to improve dynamic fidelity in HWIL simulation. Q. Liu, et al.[5] suggested a novel feedforward control scheme on the basis of Padé approximation to deal with non-minimum phase digital servo system, which could ensure small phase errors and gain errors in the low frequency range. Q. Fu, et al.[6] developed a combined control method that implants the quantitative feedback theory (QFT) into the zero phase error tracking controller. It dispenses with flaws of QFT control system and achieves high performance robustness and wide frequency bandwidth. J. Y. Yu, et al.[7] worked out an improved QFT method that made tradeoff between frequency performance indices of nominal plant and those of system uncertainty.

All of the above-mentioned studies are carried out on the basis of given system uncertainty, which is not always tenable in actual controller design. This artical describes a model-free compound controller design method. It acquires QFT experiment plant templates from the measured time response data of simulators, while converts the indices of magnitude-frequency characteristics of flight simulators to QFT-based tracking specification bounds and uses feedforward controller to satisfy the requirements for phase-fre-

*Corresponding author. Tel.: +86-451-86402748.
E-mail address: zhifuguo@126.com

doi: 10.1016/S1000-9361(08)60153-3

quency characteristics.

2. Indirect Closed-loop Identification of QFT Experiment Plant Templates Using Power Spectrum Estimation

2.1. Principles of power spectrum estimation

Assume that H is a linear time-invariant system. The cross correlation function of input signal $X(n)$ and output signal $Y(n)$ is defined as

$$R_{XY}(m)=E\{X(n)Y(n+m)\}=R_X(m)*h(m) \quad (1)$$

where $R_X(m)$ denotes auto correlation function of $X(n)$, and $h(m)$ impulse response of system H. Its Fourier transform abides by

$$P_{XY}(\omega)=P_X(\omega)H(\omega) \quad (2)$$

where $P_{XY}(\omega)$ is the cross power spectrum function of input and output signals, and $P_X(\omega)$ the power spectrum of input signal. The identification result of transfer function $H(\omega)$ can be calculated by

$$H(\omega)=\frac{P_{XY}(\omega)}{P_X(\omega)} \quad (3)$$

Since the output to be measured is likely to be corrupted by noise $N(n)$, the cross correlation function of input signal and output signal can be defined as

$$R_{XY}(m)=E[X(n)*(Y(n+m)+N(n+m))]=$$
$$R_X(m)*h(m)+R_{XN}(m) \quad (4)$$

Its corresponding Fourier transform is shown as follows:

$$P_{XY}(\omega)=P_X(\omega)H(\omega)+P_{XN}(\omega) \quad (5)$$

The reliability of Eq.(3) may then be estimated by computation of the coherence function given by[8]

$$\gamma^2(\omega)=\frac{P_{XY}(\omega)P_{XY}^*(\omega)}{P_{XX}(\omega)P_{YY}(\omega)}=\frac{|P_{XY}(\omega)|^2}{P_{XX}(\omega)P_{YY}(\omega)} \quad (6)$$

The results that stem from comparison of coherence function with the transfer function evaluated over the frequency range of interest are usually acceptable, if $\gamma^2(\omega)$ remains consistently high, i.e., $0.8<\gamma^2(\omega)<1.0$.

2.2. Indirect closed-loop identification method

Fig.1 shows the closed-loop system under consideration in a block diagram form. $P(s)$ denotes the system plant under test with output being $Y(s)$, input $X(s)$ and disturbance $N(s)$. Mathematically, the system can be described by

$$Y(s)=\frac{G(s)P(s)}{1+G(s)P(s)}X(s)+\frac{1}{1+G(s)P(s)}N(s) \quad (7)$$

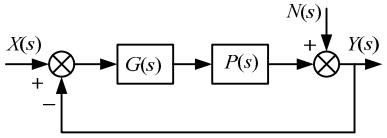

Fig.1 Schematic diagram of indirect closed-loop identification method.

The closed-loop system transfer function can be described by

$$H(s)=\frac{Y(s)}{X(s)}=\frac{G(s)P(s)}{1+G(s)P(s)} \quad (8)$$

Then, according to Eq.(8), the parameters of $P(s)$ can be estimated through open-loop system identification methods, in which the transfer function of controller in use is usually known. As for QFT experiment plant templates, the frequency data model that is built up with frequency responses in different frequency ranges is desirable. Hence, the estimated open-loop system frequency characteristic $\hat{P}(\mathrm{j}\omega)$ is given by

$$\hat{P}(\mathrm{j}\omega_i)=\frac{H(\mathrm{j}\omega_i)}{(1-H(\mathrm{j}\omega_i))G(\mathrm{j}\omega_i)} \quad (i=1,2,\cdots,n) \quad (9)$$

The advantage of indirect closed-loop system identification lies in its ability of converting closed-loop system identification into open-loop one, thereby avoiding the pitfalls inherent in closed-loop method.

2.3. Experimental conditions

In the experiments the test signal $X(t)$ is defined as

$$X(t)=A\sin\{2\pi t(f_i+0.1F(t,t_i,f_i))\}$$
$$(f_i=0.1,0.2,\cdots,40.1\ \mathrm{Hz}) \quad (10)$$

where A is the amplitude of input signal, f_i the current signal frequency, t_i the shift time from f_{i-1} to f_i and t the present time.

$$F(t,t_i,f_i)=\begin{cases}1 & (t-t_i-4/f_i)\geq 0\\ 0 & (t-t_i-4/f_i)<0\end{cases} \quad (11)$$

The frequency of input signal that lasts for four times the period of every present frequency changes from 0.1 Hz to 40.1 Hz. In this way, steady-state output response can be ensured, which is very important for power spectrum estimation. Besides, the output response of system indicates that the frequency range of input signal, [0.1, 40.1] Hz, covers the interested frequency range of system.

The angle of operating point under test is chosen between −40° and +40° with intervals of 2° each. This is done because the parameters in a real system depend continuously on the set of operating points if the angle intervals are chosen small enough. The alteration continuity of gains and phases of the system can be displayed on the Nichols chart. Each system template at the identical frequency form one disk shape, while at different frequencies, the system templates change continuously from high to low, and the gain and phase decrease with the frequency increasing. Therefore, templates of unmeasured operating points must lie in the vicinity of the neighboring templates of the measured operating point, if measured QFT experiment plant templates meet the above conditions. Furthermore, controllers designed based on the measured plant templates can also satisfy the requirements specified by the closed-loop system in the whole angle range, [−40°, +40°].

Fig.2 shows the QFT experiment plant templates obtained by using the above method, where, in order to save calculation time, redundant templates that form the same specification bounds have been deleted.

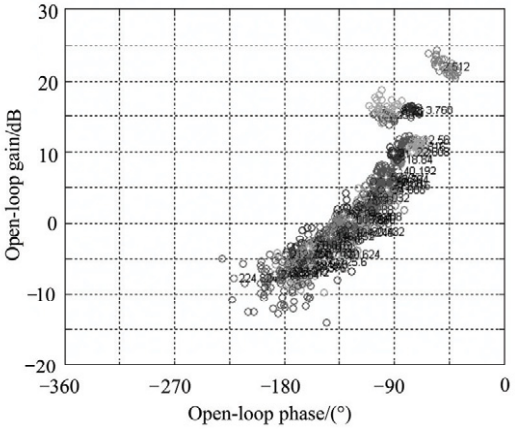

Fig.2 QFT experiment plant templates.

3. QFT Performance Bounds

QFT performance bounds are calculated based on the performance indices of flight simulator inner frame. They are determined as follows.

(1) Relative stability: Gain-margin 5 dB, and phase-margin 50°.

(2) Frequency bandwidth: The frequency of output responses of system to peak-to-peak 1° of input signal satisfies $\omega_{\pm 10^\circ} \le 6$ Hz and $\omega_{\pm 10\%} \le 6$ Hz. This means that magnitude ratio of closed-loop system should be located at [–0.915 2, 0.828 0] ($\pm 10\%$) and phase angle should be less than 10° over the frequency range below 6 Hz.

Corresponding QFT frequency domain specification bounds are as follows.

Robust margins bound is

$$\left| F \frac{PGH}{1+PGH} \right| \le W_{\mathrm{s1}}$$

Tracking bounds are

$$W_{\mathrm{s7a}} \le \left| F \frac{PG}{1+PGH} \right| \le W_{\mathrm{s7b}}$$

where F denoting the pre-filter is assumed to be $F = 1$, when controller bounds are computed, $W_{\mathrm{s1}} = 1.2$, lower bound $W_{\mathrm{s7a}} = 0.9$, upper bound $W_{\mathrm{s7b}} = 1.1$, and $\omega \le 37.7$ rad/s.

4. Controller Design (Loop Shaping)

4.1. Forward channel controller design with QFT

The job of forward channel controller is to reduce the difference between the plant's minimum and maximum outputs due to plant uncertainty, and at the same time ensure meeting the closed-loop specification. QFT controller design on Nichols chart is to make sure that every frequency response data of nominal plant denoted by small circles, lies above or on corresponding bounds. Basic transfer functions of QFT MATLAB toolbox are[9]:

(1) Simple gain, k, which serves to increase nominal plant by $20\lg k$ dB if $20\lg k > 0$ dB or decrease it if $20\lg k < 0$ dB;

(2) Simple pole or zero, $p/(s+p)$ or $(s+p)/p$, a simple pole located at $-p$ increasing the nominal plant by $-10\lg(1+\omega^2/p^2)$ dB and the phase by $-\arctan(\omega/p)$ deg;

(3) Simple lead or lag, $(s+a)/(s+b)$, with the maximum or minimum phase of a lead or a lag element appearing at $\omega = \sqrt{ab}$ and accounting to $\phi = 90^\circ - 2\arctan\sqrt{a/b}$;

(4) Second-order pole or zero, $\omega_{\mathrm{n1}}^2/(s^2 + 2\xi\omega_{\mathrm{n1}}s + \omega_{\mathrm{n1}}^2)$, $(s^2 + 2\xi\omega_{\mathrm{n1}}s + \omega_{\mathrm{n1}}^2)/\omega_{\mathrm{n1}}^2$, of which the phase and gain drop or soar from the natural frequency ω_{n1} while these elements cause small lag or lead at low frequency and $\xi = 0.5$-0.7 in general;

(5) Notch filter, $(s^2 + 2\xi_1\omega_{\mathrm{n2}}s + \omega_{\mathrm{n2}}^2)/(s^2 + 2\xi_2 \cdot \omega_{\mathrm{n2}}s + \omega_{\mathrm{n2}}^2)$, which compensates mechanical vibration due to flexibility of structures or eliminates operating frequency disturbance. ω_{n2} is the natural frequency of the notch, and ξ_2/ξ_1 determines the depth and width of the notch.

QFT controller loop shaping result is shown in Fig.3, and Curve 1 is the nominal plant. After several adjustment iterations, forward channel controller can be finally developed as

$$G(s)=2.195\frac{(s/3.243+1)}{s(s/24.48+1)}\bullet\frac{(s/29+1)}{(s/1\,000+1)} \tag{12}$$

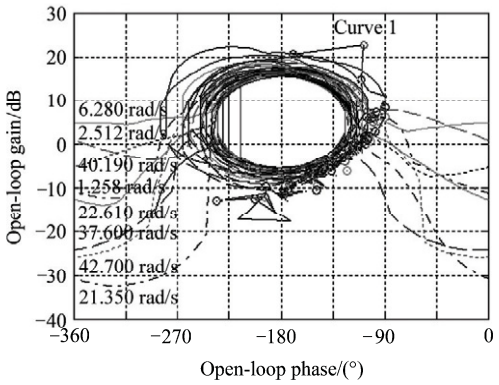

Fig.3 QFT controller loop shaping.

4.2. Feedforward controller design

Although QFT forward controller meets specified magnitude-frequency characteristics, it fails to satisfy specified phase angle characteristics at the same time. Thus, feedforward controller is required to compensate the phase angle lag. Feedforward controller is attained after adjustments as follows:

$$G_{\mathrm{f}}(s)=\frac{0.01s}{0.01s/10+1} \tag{13}$$

In the controller design, there are two rules that govern the combined controller. They are: ① On the one hand the forward channel controller must meet specified closed-loop system characteristics, such as stability, as far as possible, while on the other the feedforward controller, as an open-loop controller itself, is no concern of closed-loop performance. ② The controller must be constructed as simple as possible.

Fig.4 shows open-loop and closed-loop system frequency characteristics with and without a feedforward controller.

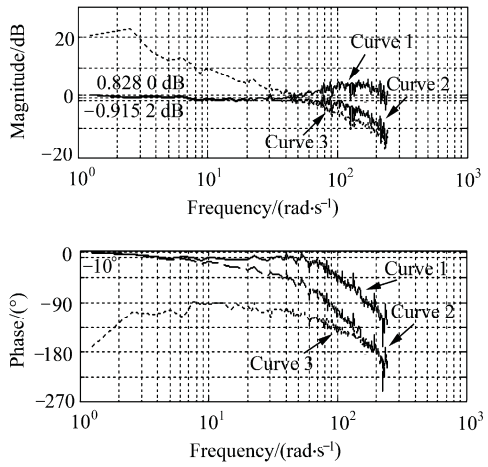

Fig.4 System frequency characteristic Bode diagram.

In Fig.4, Curve 1 shows the closed-loop frequency characteristics with a feedforward controller while Curve 2 those without a feedforward controller. Curve 3 presents the open-loop system characteristics. Curve 1 reveals that its magnitude and phase mainly lie in [−0.915 2, 0.828 0] dB and [−10°, 0°] respectively over the frequency range $\omega\in[0, 37.7]$ rad/s .

5. Experiments

In order to verify the proposed model-free compound controller design method, experiments on different controllers were carried out on a hydraulic three-axis flight simulator inner frame with peak-to-peak 1° sine wave signal and 0.005 (°)/s ramp signal. Due to inevitable measuring errors of frequency characteristics, the real parameters of the forward controller and the feedforward controller on the simulator should be subject to some adjustment.

Real controllers designed by using the model-free compound controller design method are as follows.

Forward channel controller is

$$G(s)=5\frac{(s/3.974+1)}{s(s/30+1)}\bullet\frac{(s/29+1)}{(s/1\,000+1)} \tag{14}$$

Feedforward controller is

$$G_{\mathrm{f}}(s)=\frac{0.035s}{0.035s/10+1} \tag{15}$$

The original controllers of flight simulator inner frame are as follows.

Forward channel controller is

$$G'(s)=55\frac{(s/3+1)}{(s+1)}\bullet\frac{(s/117+1)}{(s/312.5+1)}+\frac{0.05}{s}+80s \tag{16}$$

Feedforward controller is

$$G'_{\mathrm{f}}(s)=23s \tag{17}$$

Fig.5 illustrates the output time responses of flight simulator inner frame with different controllers to a 6 Hz sine wave signal. Dot line 1 represents the input sine wave signal while solid line 3 the output tracking signal of system with controllers designed by using the proposed method. Peak of the output is 0.549 3° and the magnifying ratio of magnitude |0.549 3 –0.5|/0.5 < 9.86%. Time lag at 0° is 0.000 6 s and the corresponding phase angle lag 0.004 5×360=1.296° < 10°. Therefore, the system output response shows convergence with design performance indices.

Dash dot line 2 represents the output tracking signal of system with original controllers of simulator. Peak of the output is 0.537 9° and the magnifying ratio of magnitude |0.537 9 – 0.5|/0.5 < 7.58%. Time lag at 0° is 0.007 s and the corresponding phase angle lag 0.007×6×360 = 15.12° > 10°. This means output response of the system with original controllers cannot satisfy system performance indices at ω = 6 Hz.

By comparison of output responses to sine wave inputs from the systems with different controllers, it is clear that system with controllers designed by using the proposed method has a wider frequency bandwidth.

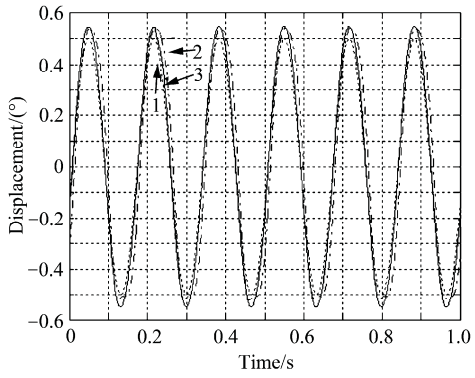

Fig.5 Response of flight simulator inner frame with different controllers to a 6 Hz sine wave signal.

Fig.6 shows output time responses to a 0.005 (°)/s ramp signal with different controllers. In it, dot line 1 is input ramp signal, dash dot line 3 output tracking signal with controllers designed by using proposed method, solid line 2 output tracking signal with original controllers, and dashed lines 4 and 5 the tolerance error of the system to 0.005 (°)/s ramp signal[10]. It can be concluded that controllers designed by proposed method also improve low-speed performance of the system as the original controllers do.

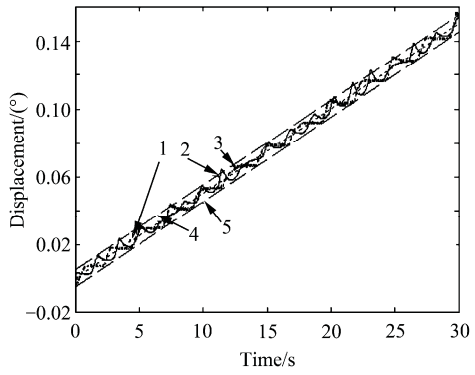

Fig.6 Response of flight simulator inner frame with different controllers to 0.005 (°)/s ramp signal.

6. Conclusions

This article presents the design procedure of model-free compound controller design method, which is based on QFT. The features of the method can be concluded as follows:

(1) Model-free. Plant templates that are set of frequency response data are identified through power spectrum estimation. Parameterized models are not necessary.

(2) Transparency. Since the controllers are designed on Nichols graph or Bode graph with QFT toolbox, design trade-offs are highly transparent between stability, performance and plant uncertainty, compared with proportion-integration-differentiation (PID) controller design method.

(3) Practicability. Simulation and experimental results indicate that the controllers designed with the proposed method can meet the performance specification of flight simulator; meanwhile, the difference between controllers used in simulation and experiment is small. The proposed method can greatly save time spent on controller design.

References

[1] Li Z M. The research on widening the band for three-axis flight simulation table. Aerospace Control 2000(2): 10-15. [in Chinese]

[2] Li Z M, Xu G B. The application of the command shaping technique in a flight simulation table. Aerospace Control 1999(4): 31-37. [in Chinese]

[3] DeMore L A, Mackin P R, Swamp M, et al. Improvements in flight table dynamic transparency for hardware-in-the-loop facilities. Proceedings of SPIE. 2000; 4027: 101-112.

[4] Swamp M, Stevens C, Hoffstetter P. Improvements in transient fidelity of HWIL flight tables using acceleration feedback. Proceedings of SPIE. 2002; 4717: 32-45.

[5] Liu Q, Feng S T, Er L J. A novel digital feedforward control of flight motion simulator. Systems Engineering and Electronics 2004; 26(10): 1460-146. [in Chinese]

[6] Fu Q. A reasearch about QFT based robust control of high performance flight simulator. PhD thesis, Beijing University of Aeronautics and Astronautics, 2004; 84-89. [in Chinese]

[7] Yu J Y. Performance analysis and experiment research for hydraulic simulator based on quantitative feedback theory. PhD thesis, Harbin Institute of Technology, 2006; 63-65. [in Chinese]

[8] Watton J. Fluid power systems. New York: Prentice Hall, 1988; 213-214.

[9] Yaniv O. Quantitative feedback design of linear and nonlinear control systems. Massachusetts: Kluwer Academic Publishers, 1999; 49-50.

[10] Chen X L, Zhang F E. Research of low-speed for simulation rotating table. Journal of Astronautics 1995; 16(4): 66-69. [in Chinese]

Biography:

Guo Zhifu Born in 1981, he received B.S. degree from Taiyuan University of Technology in 2003, and M.S. degree from Northeastern University in 2006. Currently, he is a Ph.D. candidate in Harbin Institute of Technology. His main research interests include application of quantitative feedback theory (QFT) and hydraulic servo control system.
E-mail: zhifuguo@126.com